



Relationship between extinction magnitude and climate change during major marine and terrestrial animal crises

Kunio Kaiho

Department of Earth Science, Tohoku University, Aoba-aza, Aramaki, Aoba-ku, Sendai 980-8578, Japan

Correspondence: Kunio Kaiho (kunio.kaiho.a6@tohoku.ac.jp)

Received: 28 January 2022 – Discussion started: 11 February 2022

Revised: 15 June 2022 – Accepted: 16 June 2022 – Published: 22 July 2022

Abstract. Major mass extinctions in the Phanerozoic Eon occurred during abrupt global climate changes accompanied by environmental destruction driven by large volcanic eruptions and projectile impacts. Relationships between land temperature anomalies and terrestrial animal extinctions, as well as the difference in response between marine and terrestrial animals to abrupt climate changes in the Phanerozoic, have not been quantitatively evaluated. My analyses show that the magnitude of major extinctions in marine invertebrates and that of terrestrial tetrapods correlate well with the coincidental anomaly of global and habitat surface temperatures during biotic crises, respectively, regardless of the difference between warming and cooling (correlation coefficient $R = 0.92\text{--}0.95$). The loss of more than 35 % of marine genera and 60 % of marine species corresponding to the so-called “big five” major mass extinctions correlates with a $> 7^\circ\text{C}$ global cooling and a $7\text{--}9^\circ\text{C}$ global warming for marine animals and a $> 7^\circ\text{C}$ global cooling and a $> 7^\circ\text{C}$ global warming for terrestrial tetrapods, accompanied by $\pm 1^\circ\text{C}$ error in the temperature anomalies as the global average, although the amount of terrestrial data is small. These relationships indicate that (i) abrupt changes in climate and environment associated with high-energy input by volcanism and impact relate to the magnitude of mass extinctions and (ii) the future anthropogenic extinction magnitude will not reach the major mass extinction magnitude when the extinction magnitude parallelly changes with the global surface temperature anomaly. In the linear relationship, I found lower tolerance in terrestrial tetrapods than in marine animals for the same global warming events and a higher sensitivity of marine animals to the same habitat temperature change than terrestrial animals. These phenomena fit with the ongoing extinctions.

1 Introduction

There are two habitat realms for animals: marine and terrestrial realms. Major mass extinctions of animals have occurred five times: 444, 372, 252, 201, and 66 million years ago after fundamental animal diversification was finished at ~ 520 Ma, commonly marked by high extinction percentages of animals inhabiting the marine realm (Sepkoski, 1996; Bambach, 2006; Stanley, 2016; Fan et al., 2020); these events were driven by large volcanic eruptions and projectile impacts (Schulte et al., 2010; Davies et al., 2017; Burgess et al., 2017; Bond and Grasby, 2020; Kaiho et al., 2016, 2021a, b, 2022). The last three mass extinctions after the initial diversification of tetrapods at ~ 300 Ma had high extinction percentages for terrestrial tetrapods (Sahney et al., 2010; Benton et al., 2013) and marine animals (Sepkoski, 1996; Bambach, 2006; Stanley, 2016; Fan et al., 2020). These major biotic crises were related to abrupt global climate changes (Balter et al., 2008; Korte et al., 2009; Finnegan et al., 2011; Chen et al., 2011, 2016; Vellekoop et al., 2014; Kaiho et al., 2016, 2022; Black et al., 2017) and the accompanying environmental changes, such as acid rain, ozone depletion, reduced sunlight, and oceanic anoxia, driven by large volcanic eruptions and projectile impacts (Schulte et al., 2010; Bond and Grasby, 2020). However, the relationship between climate change and terrestrial and marine animals has not been quantitatively studied.

Recently, Song et al. (2021) showed that a good relationship ($R = 0.63$) between temperature change and marine extinction magnitude under uniform time intervals (averaging ~ 10 Myr) spanning the late Ordovician (~ 450 Ma) to the early Miocene (~ 15 Ma). However, the coincidence of temperature change and extinction magnitude is unclear. Long-term surface temperature changes did not cause mass extinc-

tions because animals migrated to survive (McPherson et al., 2022). On the other hand, abrupt high-energy input by volcanism and impact on the Earth's surface caused abrupt climate changes accompanied by abrupt environmental destruction, leading to animal crises. I used only data sets of coincidental abrupt climate changes for biotic crises. I analyzed the five major mass extinctions, as well as the late Guadalupian crisis, which is considered a major mass extinction in some literature (Stanley and Yang, 1994; Rampino and Shen, 2019). The other minor crises are omitted because they remain to be studied in detail, especially the coincidence between biotic crises and climate changes.

On the modern Earth, an ongoing species extinction is occurring mainly on land rather than the sea (Barnosky et al., 2011). In addition, a study on thermal tolerance of modern animals shows a higher sensitivity of marine animals to warming than terrestrial animals (Pinsky et al., 2019). However, whether this relationship holds for ancient animals has not yet been clarified. Song et al. (2021) claimed that the sea surface temperature (SST) increase of 5.2 °C above the pre-industrial level at present rates of increase would likely result in mass extinction comparable to that of the major Phanerozoic events, regardless of other, non-climatic anthropogenic changes that negatively affect animal life. However, the global surface temperature anomaly is much higher than the SST anomaly of 5.2 °C (Kaiho and Oshima, 2017).

I aimed to clarify the relationship between the magnitude of biotic crises in not only marine invertebrates but also terrestrial vertebrates (tetrapods) and the global and habitat (marine or terrestrial realm) surface temperature anomalies using only biotic crises coinciding with abrupt climate changes to access similarity and difference in the response of terrestrial and marine animals to global and habitat (land and sea) temperature anomalies and coincidental environmental changes.

2 Data and methods

2.1 Diversity reduction percentage

Although Song et al. (2021) analyzed extinction data compared to sea surface temperature (SST) changes, there is no confirmation of the exact coincidence between extinction rate and temperature change for minor extinctions. I used only data showing the coincidence of shallow marine extinctions and temperature changes from the same outcrop of sedimentary rocks for a more accurate result. Therefore, I analyzed the six mass extinctions and the modern extinction, which coincided with global climate changes. For the five major mass extinctions, I used three marine genus loss percentage data sets based on three different methods (well-preserved genus data of Sepkosky, 1996; Bambach, 2006; Stanley, 2016). They show that the largest loss percentage occurred at the end of the Permian (58 %–66 %), the smallest

loss at the Frasnian–Famennian boundary (F–F; 18 %–41%), and intermediate loss percentage at the other three mass extinctions (39 %–52 %) (Fig. 1a). The error for genus and species loss percentages is approximately $\pm 5\%$ for $> 15\%$ loss values (Stanley, 2016). I do not use their data for the end of the Guadalupian because the uncertain high loss percentage likely due to “smear back” (Signor–Lipps effect) from the great end-Permian event is enhanced by the loss of record from lower sea level in the later Permian (Bambach, 2006) (Fig. 1a, Table 1). Instead, I use the marine species and genus diversity data of Fan et al. (2020) for the end of the Guadalupian, which seems to be the most believable data because their sedimentary rock sequences of the GSSP (Global Stratotype Section and Point) section and nearby sections contain continuous sedimentary rocks without a time gap (Fan et al., 2020; Huang et al., 2019). The data from China are likely not affected by the Signor–Lipps effect. I also used data of percentage extinction of Barnosky et al. (2011) and Ceballos et al. (2015) for the Holocene–Anthropocene (H–A) marine and terrestrial species.

I calculated percentage extinction using the marine animal diversity data of Fan et al. (2020) for the end-Guadalupian (end-G) extinction and terrestrial tetrapod diversity data of Benton (2013) and Sahney and Benton (2017) for the last four crises since the early diversification of terrestrial tetrapods in the Carboniferous. The genus (species) loss percentage is calculated using the formula of total number of extinction genera (species) for a mass extinction interval divided by total number of genera (species) in a substage just before the extinction (conventional method in Stanley, 2016).

Tetrapod genus losses of Benton (2013) and Sahney and Benton (2017) are used to represent reduction percentage for terrestrial animals because it is difficult to obtain good data for diversity losses among insects and plants. The tetrapod species data were converted from genus extinction percentage to species extinction percentage using the relationship curve between family and genera for tetrapods in Fig. 1c since the actual marine family–genus data mostly fit the conversion relationship curve of genus–species of Stanley (2016) (Fig. 1b, c).

2.2 Surface temperature anomaly

The largest absolute sea surface temperature (SST) anomalies during each crisis were obtained from the oxygen isotope ratios ($^{18}\text{O}/^{16}\text{O}$) of marine animal fossils (Balter et al., 2008; Korte et al., 2009; Finnegan et al., 2011; Chen et al., 2011) and the organic biomarker index (TEX₈₆) (Vellekoop et al., 2014) (Table 1). All the SST data are from low latitudes (Table 2). Global surface temperature anomalies at low latitudes are always intermediate values (near average values) regardless of (i) source latitudes of greenhouse gases or aerosols blocking sunlight (Kaiho and Oshima, 2017) (Table 1) and (ii) global warming and cooling because the highest anomaly appears at middle–high latitudes in the source

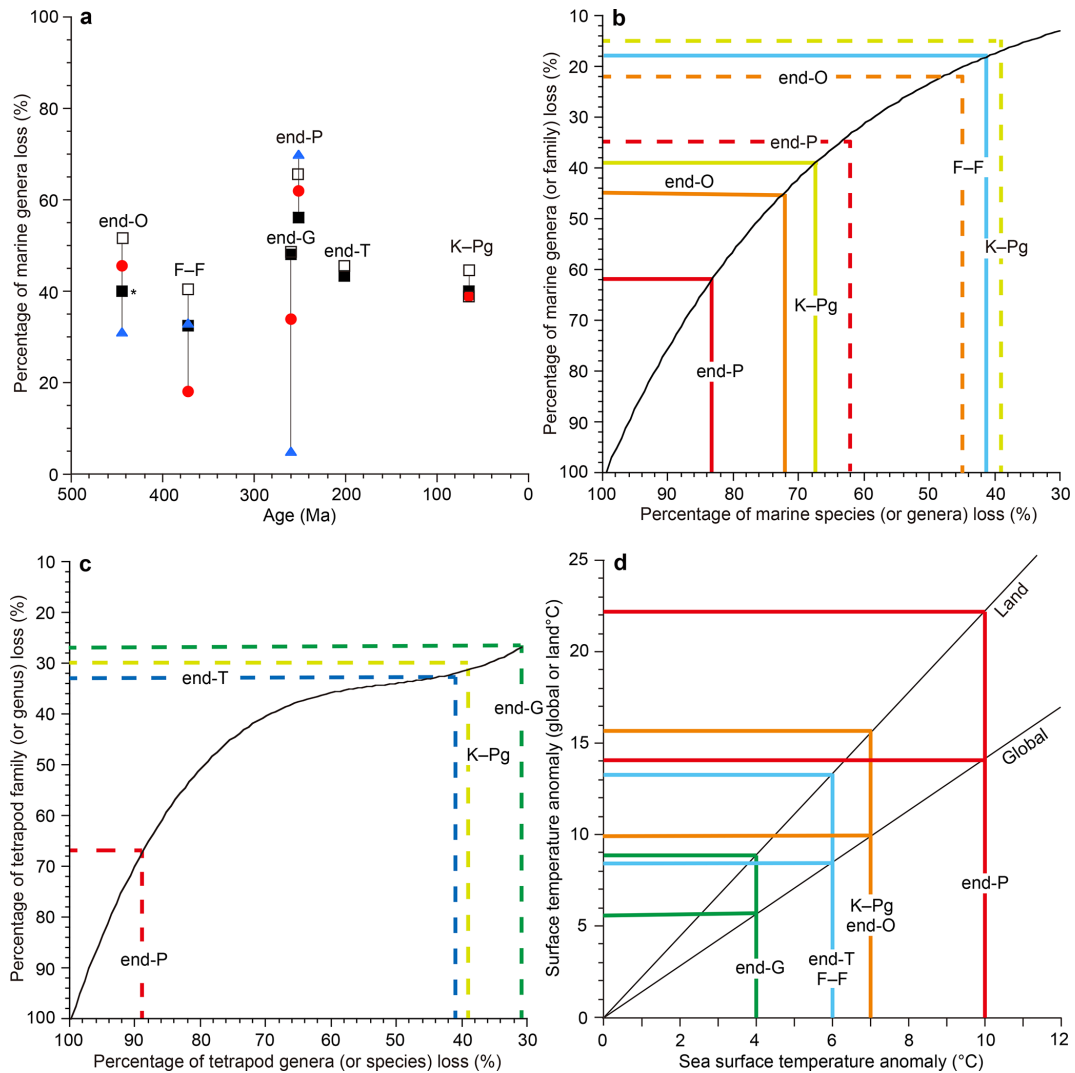


Figure 1. Marine genus loss (%) distribution (a) and relationship between extinction percentages of species, genera, and families (b for marine invertebrates, c for terrestrial tetrapods) and between global surface temperature anomalies, land-surface temperature anomalies, and sea surface temperature (SST) anomalies (d). Open square data from Sepkoski (1996), black square data from Bambach (2006), red circle data from Stanley (2016), and blue triangle data from Fan et al. (2020) in the graph (a). Graphs (b, c) were used to convert extinction percentages among species, genera, and families. Dashed lines show the genus–family loss relationship (b, c). The black curve in (b) is based on Stanley (2016). Graph (d) is based on the model calculation data from Kaiho and Oshima (2017) and is used to convert between the global surface temperature anomaly, land-surface temperature anomaly (global mean), and SST anomaly (global mean). All data are from Table 1. O: Ordovician. F–F: Frasnian–Famennian boundary. P: Permian. T: Triassic. K–Pg: Cretaceous–Paleogene boundary. The * signifies the largest extinction percentage in the Late Ordovician mass extinction (LOME).

hemisphere and the lowest anomaly appears at middle–high latitudes in the other hemisphere based on warming case data (Pinsky et al., 2019) and cooling case data (Kaiho et al., 2016). Therefore, I use each SST anomaly at low latitudes as an intermediate value (near average) on the Earth at each age. The error for the SST anomaly in geologic ages is approximately $\pm 1^\circ\text{C}$ including approximately $\pm 0.5^\circ\text{C}$ depending on the sample location to obtain the average value and approximately $\pm 0.5^\circ\text{C}$ depending on detection of the largest anomaly for abrupt short-term events from

sedimentary rocks, which are usually deposited at a rate of $1\text{--}100\text{ mm kyr}^{-1}$, except for impact ejecta sediment. I converted SST anomalies of various geologic ages to global surface temperature anomalies and land-surface temperature anomalies using Fig. 1d, which was generated from global cooling and warming (recovery) data of the climate model calculation (Kaiho and Oshima, 2017) (Fig. 1d).

Table 1. Marine animal and tetrapod family and genus extinction percentages and global, sea, and land-surface temperature anomalies.

Crisis	Age (Ma)	Marine family ext (%)	Marine genus ext (%)	Marine genus ext (%)	Marine genus ext (%)	Marine genus ext (%)	Tetrapod family ext (%)	Tetrapod genus ext (%)	Temp. anomaly (global °C)	Temp. anomaly (SST °C)	Temp. anomaly (land °C)
H–A	0	–									
K–Pg	66	15	45	40	39		30	39*	–10	–7	–16
End-T	201.4	13	46	43			33	41	–8	–6	–13
End-P	251.9	35	66	56	62	70	67	89	14	10	22
End-G	259.8	–	48	48	34	5**	27	31	6	4	9
F–F	372	–	41	35	18	33	–	–	–7	–5	–11
End-O	445–444	22*	52	40	45.5	31	–	–	10	7	16
Reference		1, 2, 3*	1	4	5	6–8*	9	10, 11*	12, 13	14–19	

Ext (%): extinction percentage. Data marked by bold and italic font are used in Fig. 3. Italic letters show values converted using Fig. 1b–d. O: Ordovician. F–F: Frasnian–Famennian boundary. G: Guadalupian. P: Permian. T: Triassic. K–Pg: Cretaceous–Paleogene boundary. The * corresponds to a reference number also marked by *. ** Data without brachiopods because their diversity increased spanning the G–L boundary. 39* at K–Pg is calculated from the data. References: 1: Sepkoski (1996); 2: Rampino et al. (2020); 3: Sepkoski (1982); 4: Bambach (2006); 5: Stanley (2016); 6: Fan et al. (2020); 7: Barnosky et al. (2011); 8: Ceballos et al. (2015); 9: Sahney et al. (2010); 10: Benton et al. (2013); 11: Sahney and Benton (2017); 12: Waters et al. (2016); 13: IPCC (2013); 14: Vellekoop et al. (2014); 15: Korte et al. (2009); 16: Chen et al. (2016); 17: Chen et al. (2011); 18: Balter et al. (2008); 19: Finnegan et al. (2011). Italic values are converted using Fig. 1b and d.

Table 2. Source latitudes of causal gas and aerosols and SST data.

Crisis	Source of causal gas and aerosols	SST data site
K–Pg	~ 25° N	~ 30° N
End-T	~ 20° S–~ 30° N	~ 30° N
End-P	~ 50° N	~ 15° N
End-G	~ 30° N	~ 30° N
F–F	~ 10° S–~ 30° N	~ 25° S
End-O	?	~ 20–~ 10° S

O: Ordovician. F–F: Frasnian–Famennian boundary. G: Guadalupian. P: Permian. T: Triassic. K–Pg: Cretaceous–Paleogene boundary.

2.3 Relationships between taxa loss percentage and temperature anomaly

Finally, I show Pearson's correlation coefficient R between taxa loss percentage and absolute habitat temperature (sea surface for marine faunas and land surface for terrestrial faunas) for the three marine genus loss percentage data sets and a terrestrial data set. To calculate their correlation coefficient, marine end-G and H–A data are included in each data set because the small percentage values cannot be changed largely due to the method variation (Table 3).

3 Results

3.1 Magnitude of marine and terrestrial crises

My analysis of the major mass extinctions shows that the Late Ordovician mass extinction (LOME) was marked by only a marine crisis (40%–52% genus loss and 68%–77% species loss in the two methods) since terrestrial tetrapods had not yet appeared. The Late Devonian mass extinction (LDME) resulted in the loss of 18%–41% of the genera and 42%–69% of the species of marine animals at the

Frasnian–Famennian boundary (F–F) (I ignored the tetrapod extinction percentage due to the very low apparent diversity) (Kaiho et al., 2016). The last three major mass extinctions, end-Permian, end-Triassic, and Cretaceous–Paleogene (K–Pg) boundary, were characterized by high extinction percentages of both marine and terrestrial genera (marine: 56%–66%, 43%–46%, and 39%–45%; terrestrial: 89%, 41%, and 39%; Fig. 2, Table 1) and species (marine: 80%–86%, 70%–73%, and 68%–72%; terrestrial: 97%, 70%, 67%; Fig. 2, Table 1). In total, the five major mass extinctions were marked by high marine genus and species extinction percentages (18%–62% and 35%–83%). However, the end-Guadalupian extinction was marked by low marine genus and species loss (5% and 11%) and higher terrestrial genus and species loss (31% and 38%), corresponding to a major terrestrial crisis, not a major mass extinction, accompanied by a large reduction in shallow marine fusulinids (Feng et al., 2020) and reef animals (Flügel and Kiessling, 2002) due to terrestrial disturbance. The Paleozoic biotic crises during global warming following the diversification of tetrapods had higher extinction percentages of terrestrial animals than of marine animals, but the Mesozoic biotic crises during global cooling had similar percentages of terrestrial and marine animals.

3.2 Sea surface temperature anomaly during crises

There are two extinction levels in the LOME at the Katian–Hirnantian boundary (445.2 Ma) and late Hirnantian (~ 444 Ma) (Bond and Grasby, 2020). Between the two extinctions, global cooling occurred, as evidenced by conodont apatite oxygen isotopes and glacial deposits (Finnegan et al., 2011); however, the two extinction levels coincided with the two shorter-term global warming events based on the oxygen isotope data of conodont apatite (Bond and Grasby, 2020). I select the maximum anomaly, +7 °C SST (~ 10⁵ years),

Table 3. Marine and terrestrial genus and species extinction percentages, absolute SST anomaly, land temperature anomaly, and their Pearson's correlation coefficient *R* for Fig. 3.

Crisis	Marine Sepkoski M genus ext (%)	Marine Sepkoski M species ext (%)	Marine Bambach M genus ext (%)	Marine Bambach M species ext (%)	Marine Stanley M genus ext (%)	Marine Stanley M species ext (%)	Absolute SST anomaly (°C)	Tetrapod genus ext (%)	Tetrapod species ext (%)	Absolute land temperature anomaly (°C)
H–A	0	0	0	0	0	0	0.7	0.6	1	1.5
K–Pg	45	72	40	68	39	68	7	39	67	16
End-T	46	73	43	70			6	41	70	13
End-P	66	86	56	80	62	83	10	89	97	22
End-G	5	11	5	11	5	11	4	31	38	9
F–F	41	69	35	62	18	42	5	–	–	11
End-O	52	77	40	68	45.5	72	7	–	–	16
Correlation <i>R</i>	0.92	0.88	0.92	0.88	0.95	0.95		0.95	0.98	

Bold roman marine taxa extinction percentage data are from Sepkoski (2006) in “Sepkoski M” (method) column, Bambach (2006) in “Bambach M” column, and Stanley (2016) in “Stanley M” column. Data of extinction percentage denoted by normal font are from Fan et al. (2020) for end-G and Barnosky et al. (2011) and Ceballos et al. (2015) for H–A. Italic values are converted using Fig. 1b–d. See Table 1 for the other explanations.

from the data of Finnegan et al. (2011) for the LOME. The trigger is estimated to be volcanism, as evidenced by coincidental mercury concentration for LOME (Jones et al., 2017; Bond and Grasby, 2020).

The LDME is composed of the Frasnian, Kellwasser, and Hangenberg crises at 383, 372, and 359 Ma, respectively, and the Kellwasser is the largest crisis (Barash, 2016). The trigger was the large igneous province (LIP) emplacement of Viluy and PDD (Pripyat–Dnieper–Donets) LIPs, as evidenced by mercury and coronene concentrations (Racki, 2020; Kaiho et al., 2021b). I use the largest abrupt cooling marked by a -5°C SST anomaly ($\sim 10^4$ years) at the lower Kellwasser and the upper Kellwasser crises from the oxygen isotope data of conodont apatite of Balter et al. (2008) for LDME, whereas the long-term gradual SST change between the crises shows global warming ($+6^{\circ}\text{C}$ SST anomaly in 5×10^5 years).

The Late Guadalupian crisis (LGC) occurred in the mid-Capitanian, at 262 Ma, followed by the Guadalupian–Lopingian (G–L) boundary event at 259 Ma (Chen and Xu, 2019). The coincidental volcanic eruptions of the Emeishan large igneous province (ELIP) in South China are thought to be the trigger of the crisis (Chen and Xu, 2019), as evidenced by mercury concentration peaks beginning in the mid-Capitanian and peaking during the G–L transition (Grasby et al., 2016). The largest abrupt anomaly, $+4^{\circ}\text{C}$ SST ($\sim 10^5$ years), coinciding with the volcanism and extinction at the G–L boundary from the data of Chen et al. (2011), is used for LGC.

The largest biodiversity loss in the Phanerozoic occurred at the end of the Permian, with local extinction during the earliest Triassic, ~ 252.0 – 251.9 million years ago (Song et al., 2013; Kaiho et al., 2021a), marking the end of the Paleozoic. The LIP in Siberia caused sill emplacement and large eruptions at that time (Burgess et al., 2017). The coincidence of volcanic eruption and the biotic crisis was shown using the correlation of mercury, coronene, and coal fly ash (Grasby

et al., 2011, 2013; Kaiho et al., 2021a). I use the largest anomaly, $+10^{\circ}\text{C}$ SST (2×10^4 years), from just before the mass extinction (Bed 24) to the first minimum $\delta^{18}\text{O}$ apatite value (base of Bed 27) at GSSP Meishan based on new conodont apatite $\delta^{18}\text{O}$ data showing the 2.5‰ anomaly of Chen et al. (2016) for the end-Permian mass extinction (EPME).

The age of the end-Triassic mass extinction (ETME) is estimated to be 201.564 ± 0.015 Ma, which corresponds to the emplacement of the Central Atlantic Magmatic Province (CAMP, 201.6 to 201.0 Ma) (Davies et al., 2017). The SST anomaly during the crisis is estimated as -6°C ($\sim 10^3$ years cooling during $\sim 10^4$ years) from the averaged $\delta^{18}\text{O}$ of oyster shells, assuming stable salinity, which was followed by long-term (2×10^5 years) global warming (Korte et al., 2009; Kaiho et al., 2022). There were no crises during the long-term warming (Kaiho et al., 2022). I use the -6°C anomaly for ETME, indicating global cooling.

Only the K–Pg mass extinction (KPME) at 66 Ma occurred as the result of an asteroid impact (Schulte et al., 2010). This impact produced large amounts of soot and sulfuric acid aerosols in the stratosphere by the ignition and melting of sedimentary rocks (Kaiho et al., 2016; Kaiho and Oshima, 2017). Stratospheric aerosols efficiently absorb and scatter solar radiation and reduce sunlight reaching the Earth's surface, which induces strong global cooling and a significant decrease in precipitation, particularly over equatorial areas, over 10 years, with the maximum occurring in the second year (Kaiho et al., 2016; Kaiho and Oshima, 2017). Organic biomarker TEX₈₆ values show -7°C as the SST's largest absolute anomaly during the crisis (Vellekoop et al., 2014). This SST anomaly is consistent with the -10°C global cooling estimated by climate model calculations and the survival of equatorial crocodylians (Kaiho et al., 2016). The global cooling duration is ~ 10 years based on impact-induced climate model calculations (Kaiho et al., 2016; Kaiho and Oshima, 2017). When the Deccan Traps volcanism also contributed

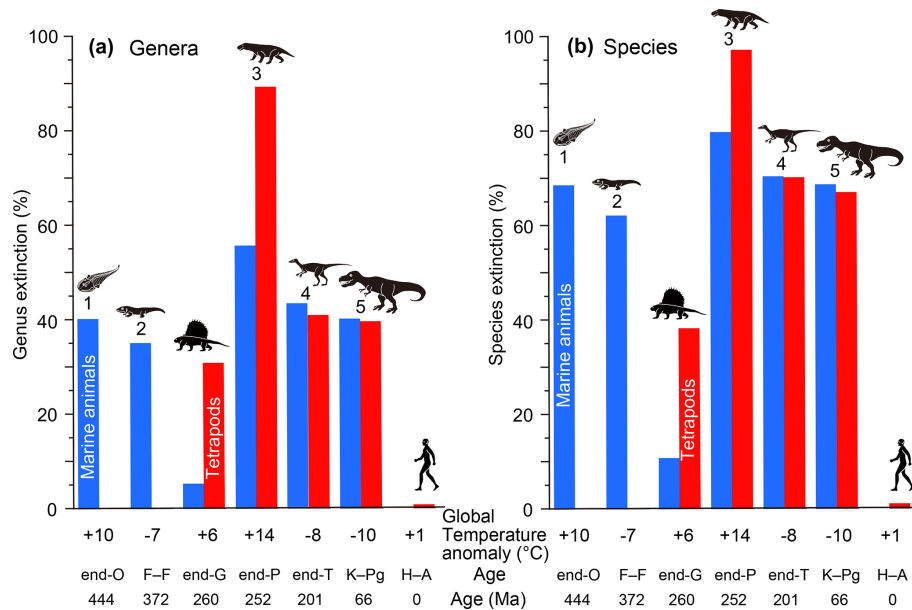


Figure 2. Genus (a) and species (b) extinction percentages of marine animals and tetrapods for major mass extinctions and the end-Guadalupian and Holocene–Anthropocene crises. All data are from Table 1. Marine genus and species extinction values shown by blue columns based on Bambach (2006) for genera and my calculation using Fig. 1b for species. Terrestrial genus and species extinction values shown by red columns based on Benton et al. (2013) and Sahney and Benton (2017) for genera and my calculations using Fig. 1b for species. These extinction percentage data are comparable because of the usage of similar methods (conventional method and substage intervals). Global temperature anomaly: global surface temperature anomaly. O: Ordovician. F–F: Frasnian–Famennian boundary. G: Guadalupian. P: Permian. T: Triassic. K–Pg: Cretaceous–Paleogene boundary. H–A: Holocene–Anthropocene (1850 to 2010 and ongoing). Numbers 1 to 5: five major mass extinctions. Each silhouette shows a representative vertebrate animal from each age.

to the global cooling, the duration could have been longer (10–10² years) for one pulse (Schmidt, 2016).

3.3 Relationship between extinction magnitudes and surface temperature anomalies

I compare those data on each biotic crisis based on an assumption that the Earth and contemporary life at the time of each crisis are themselves more-or-less comparable through time. My results for the relationship between past mass extinctions and surface temperature anomalies show the following features. A 4 °C SST warming was detected at the end of the Guadalupian (Chen et al., 2011), equivalent to 9 °C warming on land (6 °C global warming), as shown in Fig. 1d, which corresponded to 5% and 11% of marine genus and species extinctions and 31% and 38% of terrestrial genus and species extinctions, respectively (Fig. 3a, d; Table 1). The end-Ordovician mass extinction had higher temperature anomalies and higher extinction percentages (40%–46% and 68%–72% of marine genera and species, respectively). The EPME was marked by the highest temperature anomalies – 10 °C SST (Chen et al., 2016), 22 °C on land, and 14 °C global warming – and the highest extinction percentages – 56%–62% and 80%–83% of marine genera and species and 89% and 97% of terrestrial tetrapod genera and species, respectively). In contrast, the Frasnian–Famennian

(F–F) boundary, the end-Triassic, and Cretaceous–Paleogene (K–Pg) boundary mass extinctions coincided with the 5, 6, and 7 °C SST (Balter et al., 2008; Korte et al., 2009; Vellekoop et al., 2014) cooling corresponding to 11, 13, and 16 °C cooling on land and 7, 8, and 10 °C global cooling (Fig. 1). The F–F crisis corresponds to 18%–35% and 42%–62% marine genus and species loss, respectively, that is, a marine crisis and the smallest major mass extinction, respectively. The ETME correlated with 43% and 70% marine genus and species loss and 41% and 70% terrestrial tetrapod genus and species loss, respectively, and the KPME correlated with 39%–40% and 68% marine genus and species loss and 39% and 67% terrestrial tetrapod genus and species loss, respectively (Fig. 3a, d). These results indicate that a larger absolute value of the global temperature anomaly corresponds to a higher extinction percentage in the marine and terrestrial realms, regardless of whether the change is due to global warming or global cooling, considering a ±5% error (Fig. 3c, f). The correlation coefficient *R* between marine extinction percentage and absolute SST anomaly is 0.92–0.95 for genus and 0.88–0.95 for species, and that between terrestrial extinction percentage and absolute land temperature anomaly is 0.95 for genus and 0.98 for species (Fig. 3c and f, Table 3). There is little or no difference to *R* for marine animals in the three data sets. Differences in methods do not affect the conclusions. These new data indicate that

global warming temperatures ($> 9^{\circ}\text{C}$) inducing major marine extinctions are likely higher than that of global cooling ($> 7^{\circ}\text{C}$). These relationships indicate that abrupt temperature anomalies and coincidental environmental changes associated with high-energy input by volcanism and impact relate to the magnitude of mass extinctions.

4 Discussion

4.1 Summary and interpretation on extinction–temperature relationship

When summarizing and interpreting these results for the past six representative crises, I find the following four new pieces of information. (i) Higher global surface temperature anomalies correspond to higher extinction percentages in both marine and terrestrial realms (Fig. 3a, d), which suggests that climate change and related or coincidental environmental destruction are the main causes of mass extinctions on land and in the sea. (ii) $> 35\%$ genus and $> 60\%$ species loss correspond to $7\text{--}9^{\circ}\text{C}$ global warming and $> 7^{\circ}\text{C}$ global cooling for marine animals and $> 7^{\circ}\text{C}$ global cooling and $> \sim 7^{\circ}\text{C}$ global warming for terrestrial tetrapods, although the amount of terrestrial data is small (Fig. 3a, d). This relationship contains higher extinction percentages in the terrestrial realm (tetrapods) than in the marine realm (invertebrate) under the same global temperature anomaly in warming events and similar extinction percentages in the terrestrial realm (tetrapods) and the marine realm (invertebrate) in cooling events (Fig. 3a, d). The possible interpretations are (a) lower tolerance of terrestrial tetrapods for warming, (b) higher tolerance of marine animals for global warming, and (c) different ages and taxon groups. I regard the lower tolerance of terrestrial tetrapods for warming as the most likely answer because major terrestrial crises occur under lower global temperature anomalies than major marine crises in global warming (Fig. 3a, d), which implies that major terrestrial crises occurred more frequently than major marine crises evidenced by nine decreases in tetrapod diversity having $\geq 35\%$ genus loss during the late Carboniferous to Early Jurassic (Benton et al., 2013) compared with two marine crises having $\geq 35\%$ genus extinctions during the same interval (Bambach, 2006). This is consistent with the higher extinction rate of terrestrial tetrapods compared to marine animals for the current Earth; however, the consistence is due to a different cause than anthropogenic collapse of nature, which usually parallelly occurred with global warming (e.g., Waters et al., 2016), for causes of major mass extinctions. (iii) Although the ratio of the surface temperature anomaly in the terrestrial realm to that in the marine realm is 2.2 (Fig. 1d), marine animals are more likely to become extinct under a lower habitat temperature anomaly than tetrapods regardless of the difference between warming and cooling (Fig. 3c, f). This is possibly due to a higher sensitivity of marine animals to temperature

change than terrestrial animals, which have access to places of refuge based on the current global temperature and thermal tolerance data (Pinsky et al., 2019). (iv) A similar absolute habitat temperature anomaly corresponds to a similar extinction magnitude in marine animals and terrestrial tetrapods. In other words, correlation coefficient R is very high (0.92–0.95 in marine genera and 0.95 in terrestrial genera) between absolute habitat temperature anomaly and extinction magnitude (Fig. 3c, f), which indicates that the cause of the biotic crises is the surface temperature anomaly and related environmental changes.

My calculation results on extinction percentage are comparable with the genus extinction percentage data in sub-stages of Bambach and likely Sepkosky due to the usage of similar methods, whereas the Stanley method considered background extinction, which differs from my calculations; e.g., the low extinction percentage for F–F of Stanley is due to the consideration of the high background extinction percentage (Fig. 1a). I studied only biotic crises showing the coincidence of surface temperature change and an extinction, resulting in a very high correlation coefficient (0.92–0.95) between absolute SST anomaly and extinction magnitude on marine fossils in three data sets based on the three methods of Sepkosky, Bambach, and Stanley ($R = 0.92, 0.92,$ and 0.95 for genus). The correlation coefficient of Song et al. (2021) is much lower ($R = 0.63$ for genus), which is likely due to the low correlation in low extinction rates. It is likely due to the lack of sensitivity of marine animals for small temperature changes or the usage of an uncertain coincidence with global climate changes. Song et al. (2021) concluded that a temperature increase of 5.2°C above the pre-industrial level at the present rate of increase would likely result in a major marine mass extinction. The 5.2°C is the SST anomaly, which corresponds to a 7°C global surface temperature anomaly (Fig. 1d). This is consistent with my results for global cooling; however, a 9°C global surface warming is essential for a major marine mass extinction (Fig. 3a, d). The physical law of the temperature anomaly extinction relationship shown in Figs. 1d and 3 controls the extinction of terrestrial and marine animals, as shown in Fig. 2.

4.2 Climate changes and causes of mass extinctions

McPherson et al. (2022) argued that slow temperature changes will provide opportunities for species to adapt; thus, the rapidity of environmental change produced by abrupt climate change is fundamentally more important than the magnitude of the change alone for mass extinctions. The durations of global cooling and warming of the large volcanic eruptions during the five crises were 10^4 years and $10^4\text{--}10^5$ years, respectively. In the case of the cooling crises, much shorter climate change events could have repeatedly occurred because one large eruption causes a ~ 10 -year global cooling pulse (Timmreck et al., 2012). For example, a 10^4 year cool-climate period corresponding to the end-

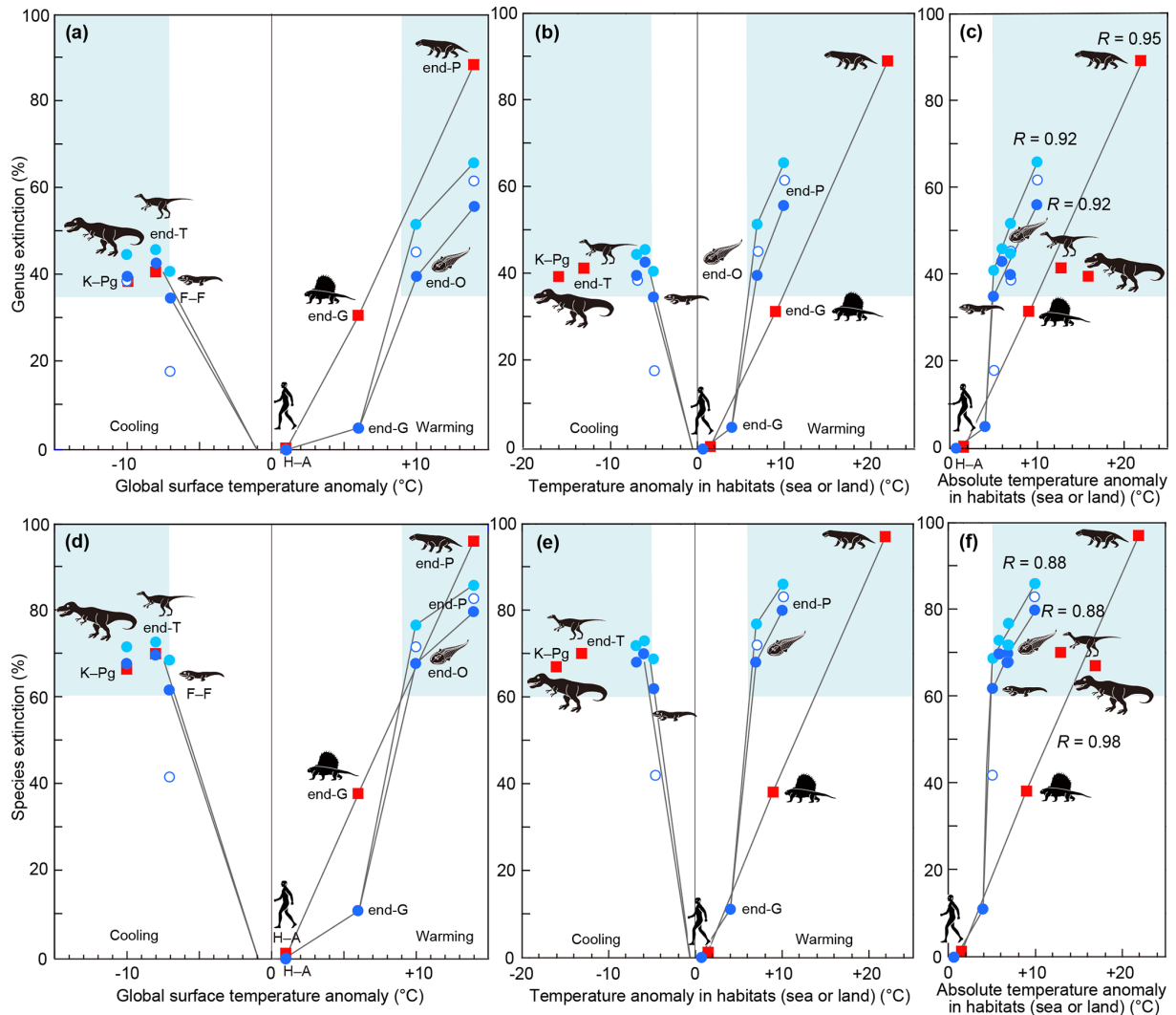


Figure 3. Relationship between genus and species extinction percentage and surface temperature anomaly in major mass extinctions, the end-Guadalupian crisis, and the current crisis in the Anthropocene. All vertical axes show genus or species extinction (%). **(a)–(c)** Genus extinction. **(d)–(f)** Species extinction. **(a, d)** Relationship between that and global surface anomaly. **(b, e)** Relationship between that and surface temperature anomaly in habitats (global sea or land). **(c, f)** Relationship between that and absolute surface temperature anomaly in habitats (global sea or land). Blue circles: marine extinctions (solid light blue circles: Sepkoski (1996; conventional method and 107 interval data points) and data of end-G and H-A; solid blue circle: Bambach (2006; conventional method and 165 substage interval data points); open circle: Stanley (2016; new method and substage interval data)). Red squares: terrestrial extinctions represented by tetrapods (calculated from data of Benton et al. (2013; substage intervals) for end-O, F-F, end-P, and end-T and Sahney et al. (2017) for K-Pg). All data are from Table 3. Comparable data sets are solid blue circles and red squares due to similar methods (conventional method and substage interval data). Pale blue areas show major extinctions. O: Ordovician. F-F: Frasnian–Famennian boundary. G: Guadalupian. P: Permian. T: Triassic. K-Pg: Cretaceous–Paleogene boundary. H-A: Holocene–Anthropocene. I also show correlation coefficient R between marine extinction percentage and absolute SST anomaly and that between terrestrial extinction percentage and absolute land temperature anomaly based on the conventional method.

Triassic mass extinction likely contained numerous cooling pulses causing the 6 °C SST reduction over 10^3 years in total (Kaiho et al., 2022). Thus volcanic eruptions cause repeated abrupt (10 years) global cooling pulses, whereas a bolide impact would cause only one cooling pulse of ~ 10 years (Kaiho et al., 2016). Global warming lasts 10^4 – 10^5 years in the case of volcanic events. Coincidental environ-

mental changes should relate to the magnitude of mass extinctions.

The significant relationship between the surface temperature anomaly and extinction magnitude indicates that the cause of major extinctions is surface temperature change and coincidental environmental changes, such as acid rain, ozone depletion, reducing sunlight, desertification, soil erosion, and

oceanic anoxia, driven by large volcanic eruptions and projectile impacts; these causal climatic and environmental conditions changed in parallel due to the same controls as each volcanism and impact. These climatic and environmental anomalies are controlled by stratospheric aerosols, such as sulfuric acid and black carbon, for reducing sunlight – global cooling – and acid rain, halogen for ozone depletion, and atmospheric greenhouse gases, such as CO₂ and methane, for surface warming.

Global cooling and warming have been reported in many periods in the Phanerozoic based on oxygen isotopes (Stanley, 2010); however, most of them are long-term climate changes. When surface temperature changes slowly ($> \sim 10^3$ years), animals migrate and survive; an abrupt temperature change and accompanying environmental change are thought to be essential for mass extinctions. There were no significant marine extinctions during global warming of two famous global warming events at the end-Cenomanian and Paleocene–Eocene transitions (Kaiho, 1994), which were due to volcanism under the oceanic crust (Bond and Wignall, 2014). This type of volcanism cannot eject volcanic SO₂ gas into the stratosphere, resulting in no short-term global cooling and gradual global warming by the gradual release of CO₂ from volcanism under the ocean; conversely, the Late Devonian, end-Permian, and end-Triassic LIPs were emplaced on land, resulting in SO₂ gas emissions into the stratosphere, causing short-term global cooling and accompanying environmental changes, followed by longer-term global-warming due to volcanic greenhouse gas emissions. An eruption causes global cooling that lasts for a few to 10 years; thus, detection is difficult. However, LIP volcanism causes thousands of eruptions (Svensen et al., 2009), resulting in the detection of decreases in SST from sedimentary rocks when the release of SO₂ gas to the stratosphere exceeds $> 10^3$ years (Kaiho et al., 2022), but no detection occurs in cases of $< 10^2$ year SO₂ emissions. Global cooling is followed by global warming due to the cessation of SO₂ release to the stratosphere and the accumulation of CO₂ in the atmosphere from volcanism (Kaiho et al., 2022). Global warming lasts for a long time (usually 10^4 – 10^5 years), resulting in easy detection.

Global warming has been detected in some volcanic and impact cases, whereas global cooling has been detected from (i) sedimentary rocks formed under volcanism characterized by massive SO₂ gas emissions and relatively low CO₂ emissions by low-temperature volcanism to the stratosphere (ETME) (Kaiho et al., 2022) and (ii) quickly deposited impact ejecta (Vellekoop et al., 2014) near the impact crater in an impact case (KPME). There is a possibility of undetected short-term global cooling before global warming in the other volcanism-induced major biotic crises. Larger volcanism generally causes larger SO₂, CO₂, and halogen emissions, which could have resulted in a significant relationship between the global warming temperature anomaly and extinction magnitude even if the real main cause of crises is

reduced sunlight (global cooling), acid rain, ozone depletion, or oceanic anoxia. Therefore, the relationship between the absolute temperature anomaly and extinction magnitude is shown in Fig. 3c and f. The significant relationship in marine and terrestrial animals clarified in this study indicates that the global climate and the accompanying environmental changes are related to the magnitude of mass extinctions. Although Song et al. (2021) claimed that a temperature increase of 5.2 °C above the pre-industrial level at present rates of increase would likely result in mass extinction comparable to that of the major Phanerozoic events, regardless of other, non-climatic anthropogenic changes that negatively affect animal life, the temperature increase is not 5.2 °C but 9 °C. The 9 °C global warming will not appear in the Anthropocene at least till 2500 under the worst scenario (IPCC, 2013; IUCN, 2021; Tebaldi, et al., 2021). Prediction of the future anthropogenic extinction magnitude using only surface temperature is difficult, because the causes of the anthropogenic extinction differ from causes of mass extinctions in geologic time. However, I can predict that the future anthropogenic extinction magnitude will not reach the major mass extinction magnitude when the future anthropogenic extinction magnitude parallelly changes to global surface temperature anomaly.

5 Conclusions

I conclude that the relationship between extinction magnitude and climate change during major marine and terrestrial animal crises is very high. There is a significant relationship ($R = 0.92$ – 0.95) between extinction magnitude of marine invertebrates and absolute SST anomaly, as well as that of terrestrial tetrapods and absolute land-surface temperature anomaly ($R = 0.95$ – 0.98). The $> 35\%$ genus and $> 60\%$ species loss correlate to a $> 7\text{ °C}$ global cooling and a 7 – 9 °C global warming for marine animals and a $> 7\text{ °C}$ global cooling and a $> \sim 7\text{ °C}$ global warming for terrestrial tetrapods. These relationships indicate that abrupt temperature anomalies and coincidental environmental changes associated with abrupt high-energy input by LIP volcanism and an asteroid impact relate to the magnitude of mass extinctions. The future anthropogenic extinction magnitude will not reach the major mass extinction magnitude when the extinction magnitude parallelly changes with global surface temperature anomaly. In the linear relationship, I found that (i) terrestrial tetrapods had a lower tolerance than marine animals for the same global warming events and (ii) marine animals have a higher sensitivity to the same habitat temperature change than terrestrial animals, which have access to places of refuge. These phenomena will appear in the coming hundred years.

Data availability. All data are available in the main text.

Competing interests. The author has declared that there are no competing interests.

Disclaimer. Publisher's note: Copernicus Publications remains neutral with regard to jurisdictional claims in published maps and institutional affiliations.

Acknowledgements. This study was supported by the Japan Society for the Promotion of Science (KAKENHI – Grants-in-Aid for Scientific Research; grant no. 25247084) for Kunio Kaiho. I thank the anonymous referees for their useful comments.

Financial support. This research has been supported by the Japan Society for the Promotion of Science (grant no. 25247084).

Review statement. This paper was edited by Petr Kuneš and reviewed by two anonymous referees.

References

- Balter, V., Renaud, S., Girard, C., and Joachimski, M. M.: Record of climate-driven morphological changes in 376 Ma Devonian fossils, *Geology*, 36, 907–910, <https://doi.org/10.1130/G24989A.1>, 2008.
- Bambach, R. K.: Phanerozoic biodiversity mass extinctions, *Ann. Rev. Ear. Planet. Sci.*, 34, 127–155, <https://doi.org/10.1146/annurev.earth.33.092203.122654>, 2006.
- Barash, M. S.: Causes of the great mass extinction of marine organisms in the Late Devonian, *Oceanology*, 56, 863–875, <https://doi.org/10.1134/S0001437016050015>, 2016.
- Barnosky, A. D., Hadly, E. A., Gonzalez, P., Head, J., Polly, P. D., Lawing, A. M., Eronen, J. T., Ackerly, D. D., Alex, K., Biber, E., Blois, J., Brashares, J., Ceballos, G., Davis, E., Dietl, G.P., Dirzo, R., Doremus, H., Fortelius, M., Greene, H. W., Hellmann, J., Hickler, T., Jackson, S. T., Kemp, M., Koch, P. L., Kremen, C., Lindsey, E. L., Looy, C., Marshall, C. R., Mendenhall, C., Mulch, A., Mychajliw, A. M., Nowak, C., Ramakrishnan, U., Schnitzler, J., Das Shrestha, K., Solari, K., Stegner, L., Stegner, M. A., Stenseth, N. C., Wake, M. H., and Zhang, Z.: Has the Earth's sixth mass extinction already arrived?, *Nature*, 471, 51–57, <https://doi.org/10.1038/nature09678>, 2011.
- Benton, M. J., Ruta, M., Dunhill, A. M., and Sakamoto, M.: The first half of tetrapod evolution, sampling proxies, and fossil record quality, *Palaeogeogr. Palaeoclimatol.*, 372, 18–41, <https://doi.org/10.1016/j.palaeo.2012.09.005>, 2013.
- Black, B. A., Neely, R. R., Lamarque, J.-F., Elkins-Tanton, L. T., Kiehl, J. T., Shields, C. A., Mills, M. J., and Bardeen, C.: Systemic swings in end-Permian climate from Siberian Traps carbon and sulfur outgassing, *Nat. Geosci.*, 11, 949–954, 2018.
- Bond, D. P. G. and Grasby, S. E.: Late Ordovician mass extinction caused by volcanism, warming, and anoxia, not cooling and glaciation, *Geology*, 48, 777–781, <https://doi.org/10.1130/G47377.1>, 2020.
- Bond, D. P. G. and Wignall, P. B.: “Large igneous provinces and mass extinctions: An update”, in: *Volcanism, Impacts, and Mass Extinctions: Causes and Effects*, edited by: Keller, G. and Kerr, A. C., *Geol. Soc. Am. Spec. Pap.* 505, 29–55, [https://doi.org/10.1130/2014.2505\(02\)](https://doi.org/10.1130/2014.2505(02)), 2014.
- Burgess, S. D., Muirhead, J. D., and Bowring, S.: Initial pulse of Siberian Traps sills as the trigger of the end-Permian mass extinction, *Nat. Comm.*, 8, 15596, <https://doi.org/10.1038/s41467-017-00083-9>, 2017.
- Ceballos, G., Ehrlich, P. R., Barnosky, A. D., García, A., Pringle, R. M., and Palmer, T. M.: Accelerated modern human-induced species losses: Entering the sixth mass extinction, *Sci. Adv.*, 1, e1400253, <https://doi.org/10.1126/sciadv.1400253>, 2015.
- Chen, J. and Xu, Y.: Establishing the link between Permian volcanism and biodiversity changes: Insights from geochemical proxies, *Gondwana Res.*, 75, 68–96, <https://doi.org/10.1016/j.gr.2019.04.008>, 2019.
- Chen, B., Joachimski, M. M., Sun, Y. D., Shem, S. Z., and Lai, X. L.: Carbon and conodont apatite oxygen isotope records of Guadalupian-Lopingian boundary sections: Climatic or sea-level signal?, *Palaeogeogr. Palaeoclimatol.*, 311, 145–153, <https://doi.org/10.1016/j.palaeo.2011.08.016>, 2011.
- Chen, J., Shen, S., Li, X., Xu, Y., Joachimski, M. M., Bowring, S. A., Erwin, D. H., Yuan, D., Chen, B., Zhang, H., Wang, Y., Cao, C., Zheng, Q., and Mu, L.: High-resolution SIMS oxygen isotope analysis on conodont apatite from South China and implications for the end-Permian mass extinction, *Palaeogeogr. Palaeoclimatol.*, 448, 26–38, <https://doi.org/10.1016/j.palaeo.2015.11.025>, 2016.
- Davies, J. H. F. L., Marzoli, A., Bertrand, H., Youbi, N., Ernesto, M., and Schaltegger, U.: End-Triassic mass extinction started by intrusive CAMP activity, *Nat. Commun.*, 8, 15596, <https://doi.org/10.1038/ncomms15596>, 2017.
- Fan, J., Shen, S., Erwin, D. H., Sadler, P. M., MacLeod, N., Cheng, Q., Hou, X., Yang, J., Wang, X., Wang, Y., Zhang, H., Chen, X., Li, G., Zhang, Y., Shi, Y., Yuan, D., Chen, Q., Zhang, L., Li, C., and Zhao, Y.: A high-resolution summary of Cambrian to Early Triassic marine invertebrate biodiversity, *Science*, 367, 272–277, <https://doi.org/10.1126/science.aax4953>, 2020.
- Feng, Y., Song, H., and Bond, D. P. G.: Size variations in foraminifers from the early Permian to the Late Triassic: implications for the Guadalupian–Lopingian and the Permian–Triassic mass extinctions, *Paleobiology*, 46, 511–532, <https://doi.org/10.1017/pab.2020.37>, 2020.
- Finnegan, S., Bergmann, K., Eiler, J. M., Jones, D. S., Fike, D. A., Eisenman, I., Hughes, N. C., Tripathi, A. K., and Fischer, W. W.: The magnitude and duration of Late Ordovician–Early Silurian Glaciation, *Science*, 331, 903–906, [10.1126/science.1200803](https://doi.org/10.1126/science.1200803), 2011.
- Flügel, E. and Kiessling, W.: Patterns of Phanerozoic reef crises, *SEPM Spec. P.*, 72, 691–733, <https://doi.org/10.2110/pec.02.72.0691>, 2002.
- Grasby, S. E., Beauchamp, B., Bond, D. P. G., Wignall, P. B., and Sanei, H.: Mercury anomalies associated with three extinction events (Capitanian Crisis, Latest Permian Extinction and the Smithian/Spathian Extinction) in NW Pangea, *Geol. Mag.*, 153, 285–297, <https://doi.org/10.1017/S0016756815000436>, 2016.
- Grasby, S. E., Sanei, H., and Beauchamp, B.: Catastrophic dispersion of coal fly ash into oceans during the latest Permian extinction, *Nat. Geosci.*, 4, 104–107, 2011.

- Grasby, S. E., Sanei, H., Beauchamp, B., and Chen, Z. H.: Mercury deposition through the Permo-Triassic biotic crisis, *Chem. Geol.*, 351, 209–216, <https://doi.org/10.1016/j.chemgeo.2013.05.022>, 2013.
- Huang, Y., Chen, Z.-Q., Wignall, P. B., Grasby, S. E., Zhao, L., Wang, X., and Kaiho, K.: Biotic responses to volatile volcanism and environmental stresses over the Guadalupian-Lopingian (Permian) transition, *Geology*, 47, 175–178, <https://doi.org/10.1130/G45283.1>, 2019.
- IPCC, 2013: Climate Change 2013, in: The Physical Science Basis, Contribution of Working Group I to the Fifth Assessment Report of the Intergovernmental Panel on Climate Change, edited by: Stocker, T. F., Qin, D., Plattner, G. K., Tignor, M. M. B., Allen, S. K., Boschung, J., Nauels, A., Xia, Y., Bex, V., and Midgley, P. M., Cambridge University Press, Cambridge, United Kingdom and New York, USA, 1535 pp., 2013.
- Jones, D. S., Martini, A. M., Fike, D. A., and Kaiho, K.: A volcanic trigger for the Late Ordovician mass extinction? Mercury data from south China and Laurentia, *Geology*, 45, 631–634, <https://doi.org/10.1130/G38940.1>, 2017.
- Kaiho, K.: Planktonic and benthic foraminiferal extinction events during the last 100 m.y., *Palaeogeogr., Palaeoclimatol., 111*, 45–71, [https://doi.org/10.1016/0031-0182\(94\)90347-6](https://doi.org/10.1016/0031-0182(94)90347-6), 1994.
- Kaiho, K. and Oshima, N.: Site of asteroid impact changed the history of life on Earth: the low probability of mass extinction, *Sci. Rep.*, 7, 14855, <https://doi.org/10.1038/s41598-017-14199-x>, 2017.
- Kaiho, K., Oshima, N., Adachi, K., Adachi, Y., Mizukami, T., Fujibayashi, M., and Saito, R.: Global climate change driven by soot at the K–Pg boundary as the cause of the mass extinction, *Sci. Rep.*, 6, 28427, <https://doi.org/10.1038/srep28427>, 2016.
- Kaiho, K., Aftabuzzaman, M., Jones, D. S., and Tian, L.: Pulsed volcanic combustion events coincident with the end-Permian terrestrial disturbance and the following global crisis, *Geology*, 49, 289–293, <https://doi.org/10.1130/G48022.1>, 2021a.
- Kaiho, K., Miura, M., Tezuka, M., Hayashi, N., Jones, D. S., Oikawa, K., Casier, J.-G., Fujibayashi, M., and Chen, Z.-Q.: Coronene, mercury, and biomarker data support a link between extinction magnitude and volcanic intensity in the Late Devonian, *Global Planet. Change*, 199, 103452, <https://doi.org/10.1016/j.gloplacha.2021.103452>, 2021b.
- Kaiho, K., Tanaka, D., Richoz, S., Jones, D. S., Saito, R., Kameyama, D., Ikeda, M., Takahashi, S., Aftabuzzaman, M., and Fujibayashi, M.: Volcanic temperature changes modulated volatile release and climate fluctuations at the end-Triassic mass extinction, *Earth Planet. Sc. Lett.*, 579, 117364, <https://doi.org/10.1016/j.epsl.2021.117364>, 2022.
- Korte, C., Hesselbo, S. P., Jenkyns, H. C., Rockaby, R. E., and Spoetl, C.: Palaeoenvironmental significance of carbon- and oxygen-isotope stratigraphy of marine Triassic–Jurassic boundary sections in SW Britain, *J. Geol. Soc.*, 166, 431–445, <https://doi.org/10.1144/0016-76492007-177>, 2009.
- McPherson, G. R., Sirmacek, B., and Vinuesa, R.: Environmental thresholds for mass-extinction events, *Results Eng.*, 13, 100342, <https://doi.org/10.1016/j.rineng.2022.100342>, 2022.
- Pinsky, M. L., Eikeset, A. M., McCauley, D. J., Payne, J. L., and Sunday, J. M.: Greater vulnerability to warming of marine versus terrestrial ectotherms, *Nature*, 569, 108–111, <https://doi.org/10.1038/s41586-019-1132-4>, 2019.
- Racki, G.: A volcanic scenario for the Frasnian–Famennian major biotic crisis and other Late Devonian global changes: More answers than questions?, *Global Planet. Change*, 189, 103174, <https://doi.org/10.1016/j.gloplacha.2020.103174>, 2020.
- Rampino, M. R. and Shen, S.-Z.: The end-Guadalupian (259.8 Ma) biodiversity crisis: the sixth major mass extinction?, *Hist. Biol.*, 33, 1–7, <https://doi.org/10.1080/08912963.2019.1658096>, 2019.
- Rampino, M. R., Caldeira, K., and Zhu, Y.: A 27.5-Myr underlying periodicity detected in extinction episodes of non-marine tetrapods, *Hist. Biol.*, 33, 3084–3090, <https://doi.org/10.1080/08912963.2020.1849178>, 2020.
- Raup, D. M.: Size of the Permo-Triassic bottleneck and its evolutionary implications, *Science*, 206, 217–218, <https://doi.org/10.1126/science.206.4415.217>, 1979.
- Sahney, S. and Benton, M. J.: The impact of the Pull of the Recent on the fossil record of tetrapods, *Evol. Ecol. Res.*, 18, 2017.
- Sahney, S., Benton, M. J., and Ferry, P. A.: Links between global taxonomic diversity, ecological diversity, and the expansion of vertebrates on land, *Biol. Lett.*, 6, 544–547, <https://doi.org/10.1098/rsbl.2009.1024>, 2010.
- Schulte, P., Alegret, L., Arenillas, I., Arz, J. A., Barton, P. J., Bown, P. R., Bralower, T. J., Christeson, G. L., Claeys, P., Cockell, C. S., Collins, G. S., Deutsch, A., Goldin, T. J., Goto, K., Grajales-Nishimura, J. M., Grieve, R. A. F., Gulick, S. P. S., Johnson, K. R., Kiessling, W., Koeberl, C., Kring, D. A., MacLeod, K. G., Matsui, T., Melosh, J., Montanari, A., Morgan, J. V., Neal, C. R., Nichols, D. J., Norris, R. D., Pierazzo, E., Ravizza, G., Rebolledo-Vieyra, M., Reimold, W. U., Robin, E., Salge, T., Speijer, R. P., Sweet, A. R., Urrutia-Fucugauchi, J., Vajda, V., Whalen, M. T., and Willumsen, P. S.: The Chicxulub asteroid impact and mass extinction at the Cretaceous–Paleogene boundary, *Science*, 327, 1214–1218, <https://doi.org/10.1126/science.1177265>, 7–23, 2010.
- Sepkoski Jr., J. J.: Mass extinctions in the Phanerozoic oceans: A review, *Geological Implications of Impacts of Large Asteroids and Comets on the Earth*, in edited by: Silver, L. T. and Schultz, Geol. Soc. Am. Spec. Pap., 190, 283–289, 1982.
- Sepkoski Jr., J. J.: Phanerozoic overview of mass extinction. Patterns and Processes in the History of Life, edited by: Raup, D. M. and Jablonski, D., Springer-Verlag, Heidelberg, Germany, 277–295, https://doi.org/10.1007/978-3-642-70831-2_15, 1986.
- Sepkoski Jr., J. J.: Patterns of Phanerozoic extinctions: A perspective from global data bases, in: *Global Event Stratigraphy*, edited by: Walliser, O. H., Springer-Verlag, Berlin, Heidelberg, Germany, 35–52, 1996.
- Song, H., Wignall, P. B., Tong, J., and Yin, H.: Two pulses of extinction during the Permian-Triassic crisis., *Nat. Geosci.*, 6, 52–56, <https://doi.org/10.1038/NGEO1649>, 2013.
- Song, H., Kemp, D. B., Tian, L., Chu, D., Song, H., and Dai, X.: Thresholds of temperature change for mass extinctions, *Nat. Comm.*, 12, 4694, <https://doi.org/10.1038/s41467-021-25019-2>, 2021.
- Stanley, S. M.: Relation of Phanerozoic stable isotope excursions to climate, bacterial metabolism, and major extinctions, *P. Natl. Acad. Sci. USA*, 107, 19185–19189, 2010.
- Stanley, S. M.: Estimates of the magnitudes of major marine mass extinctions in earth history, *P. Natl. Acad. Sci. USA*, 113, 6325–6334, 2016.

- Stanley, S. M. and Yang, X.: A double mass extinction at the end of the Paleozoic era, *Science*, 266, 1340–1344, <https://doi.org/10.1126/science.266.5189.1340>, 1994.
- Svensen, H., Planke, S., Polozov, A. G., Schmidbauer, N., Corfu, F., Podladchikov, Y. Y., and Jamtveit, B.: Siberian gas venting and the end-Permian environmental crisis, *Earth Planet. Sc. Lett.*, 277, 490–500, <https://doi.org/10.1126/science.1224126>, 2009.
- Tebaldi, C., Debeire, K., Eyring, V., Fischer, E., Fyfe, J., Friedlingstein, P., Knutti, R., Lowe, J., O'Neill, B., Sanderson, B., van Vuuren, D., Riahi, K., Meinshausen, M., Nicholls, Z., Tokarska, K. B., Hurtt, G., Kriegler, E., Lamarque, J.-F., Meehl, G., Moss, R., Bauer, S. E., Boucher, O., Brovkin, V., Byun, Y.-H., Dix, M., Gualdi, S., Guo, H., John, J. G., Kharin, S., Kim, Y., Koshiro, T., Ma, L., Olivié, D., Panickal, S., Qiao, F., Rong, X., Rosenbloom, N., Schupfner, M., Séférian, R., Sellar, A., Semmler, T., Shi, X., Song, Z., Steger, C., Stouffer, R., Swart, N., Tachiiri, K., Tang, Q., Tatebe, H., Voldoire, A., Volodin, E., Wyser, K., Xin, X., Yang, S., Yu, Y., and Ziehn, T.: Climate model projections from the Scenario Model Intercomparison Project (ScenarioMIP) of CMIP6, *Earth Syst. Dynam.*, 12, 253–293, <https://doi.org/10.5194/esd-12-253-2021>, 2021.
- Timmreck, C., Graf, H.-F., Zanchettin, D., Hagemann, S., Kleinen, T., and Krüger, K.: Climate response to the Toba super-eruption: Regional changes, *Quat. Int.*, 258, 30–44, <https://doi.org/10.1016/j.quaint.2011.10.008>, 2012.
- Vellekoop, J., Sluijs, A., Smit, J., Schouten, S., J. Weijers, W. H., Sinninghe Damsté, J. S., and Brinkhuis H.: Rapid short-term cooling following the Chicxulub impact at the Cretaceous–Paleogene boundary, *P. Natl. Acad. Sci. USA*, 111, 7537–7541, 2014.
- Waters, C. N., Zalasiewicz, J., Summerhayes, C., Barnosky, A. D., Poirier, C., Galuszka, A., Cearreta, A., Edgeworth, M., Ellis, E. C., Ellis, M., Jeandel, C., Leinfelder, R., McNeill, J. R., deB. Richter, D., Steffen, W., Syvitski, J., Vidas, D., Waples, M., Williams, M., Zhisheng, A., Grinevald, J., Odada, E., Oreskes, N., and Wolfe, A. P.: The Anthropocene is functionally and stratigraphically distinct from the Holocene, *Science*, 351, aad2622, <https://doi.org/10.1126/science.aad2622>, 2016.